

# Highly Sensitive and Optically Transparent Resistive Pressure Sensors Based on a Graphene/Polyaniline-Embedded PVB Film

Shi-Yu Liu<sup>1</sup>, Lu Lian, Jin Pan, Jian-Gang Lu, and Han-Ping D. Shieh, *Fellow, IEEE*

**Abstract**—The development of a facile, low-temperature, and low-cost method to fabricate highly sensitive and optically transparent resistive pressure sensors remains a challenge. In this paper, a graphene/polyaniline-embedded polyvinyl butyral (GPANI-PVB) composite film is employed as the active layer in a resistive pressure sensor; this film is ultrathin, highly sensitive, optically transparent, anisotropically conductive, highly durable, highly flexible, and bending insensitive. A flexible touch panel based on the GPANI-PVB composite film is fabricated using a facile process, which supports multitouch and multilevel pressure detection. The GPANI-PVB composite film offers great potential for applications in flexible and transparent interactive electronic devices.

**Index Terms**—Flexible touch panel, graphene/polyaniline-embedded polyvinyl butyral (GPANI-PVB) composite, high sensitivity, high transparency, resistive pressure sensor.

## I. INTRODUCTION

PRESSURE sensors, including capacitive, piezoelectric, and resistive types, are widely used in displays, robotics, and prosthetics [1]–[3]. For application in displays, pressure-sensitive touch panels serve as an intuitive interactive interface and provide users with touch depth perception as well as conventional contact positioning on the screen surface. Current pressure-sensitive touch technologies applied in smart phones mainly make the use of capacitive pressure sensors, such

as 3-D touch proposed by some suppliers. With a pressure applied, such touch panels can detect tiny increase in capacitance due to the reduction in distance between sensor electrodes [4]. However, they have issues of low sensitivity due to large parasitic capacitance, high susceptibility to electronic noises [3], and possible sensitivity variation due to bending for flexible display applications. Pressure-sensitive touch panels based on self-powered piezoelectric pressure sensors [5] were also reported. However, they usually cannot support the detection of static pressure and multipress, and need extra pressure sensors in addition to conventional capacitive touch sensors. Therefore, capacitive and piezoelectric pressure sensors are possibly not the best candidates for flexible pressure-sensitive touch panels.

Compared with capacitive [4], [6]–[9] and piezoelectric types [5], [10]–[12], resistive pressure sensors respond to applied pressure with a change in the resistance of the active layer. Composites consisting of insulating elastomers and conductive fillers, such as carbon nanotubes [13], [14] and silver nanowires [15], have been developed to fabricate resistive pressure sensors. Recently, microstructures, such as porous [13], pyramidal [16], and triangular [17] morphologies, have also been introduced into composites to improve the sensitivity of pressure sensors. Basically, these sensors are based on two mechanisms [3]. One uses piezoresistive elastomers whose resistivity changes with the applied pressure due to the rearrangement of conductive fillers in elastomers [13], [18], [19]. Such pressure sensors usually suffer from low sensitivity, high hysteresis, and temperature dependence of pressure sensitivity. The second mechanism achieves high sensitivity by fabricating microstructures on elastomers or electrodes to increase the relative change in contact resistance with a pressure applied [16], [17]. However, because of the abundance of conductive fillers, these two kinds of sensors usually have low transparency, hindering their application in touch panels. Recently, a transparent bending-insensitive resistive pressure sensor fabricated using an electrospinning process was proposed [20]. Although high transmittance (more than 90% in the visible-to-infrared wavelength region) can be obtained, the pressure sensor exhibits high sensitivity only in the pressure regime of less than 1 kPa, which is not applicable for pressure-sensitive touch panels (sustaining

Manuscript received December 29, 2017; revised February 9, 2018; accepted March 6, 2018. Date of publication March 21, 2018; date of current version April 20, 2018. This work was supported in part by the National Key R&D Program of China under Grant 2017YFB1002900, in part by the National Natural Science Foundation of China under Grant 61775135, and in part by the Zhejiang Firstar Panel Technology Co., Ltd. The review of this paper was arranged by Editor F. Ayazi. (*Corresponding author: Jian-Gang Lu.*)

S.-Y. Liu, L. Lian, J. Pan, and J.-G. Lu are with the National Engineering Laboratory for TFT-LCD Materials and Technologies, Department of Electronic Engineering, Shanghai Jiao Tong University, Shanghai 200240, China (e-mail: lujg@sjtu.edu.cn).

H.-P. D. Shieh is with the Display Institute, National Chiao Tung University, Hsinchu 300, Taiwan, and also with the National Engineering Laboratory for TFT-LCD Materials and Technologies, Department of Electronic Engineering, Shanghai Jiao Tong University, Shanghai 200240, China.

Color versions of one or more of the figures in this paper are available online at <http://ieeexplore.ieee.org>.

Digital Object Identifier 10.1109/TED.2018.2814204

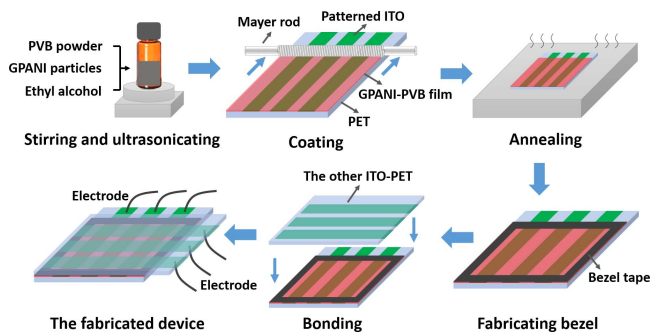


Fig. 1. Fabrication process of the GPANI-PVB composite film and the flexible touch panel.

pressures of 0–100 kPa). Moreover, the fabrication process and required equipment are complicated and challenging. Recently, a flexible and transparent resistive pressure sensor array based on percolative graphene films was reported for touch panels [21]. However, because its pressure-sensitive feature relies on the stretchability of the graphene films, the sensor array may suffer from sensitivity variation due to bending. Moreover, its fabrication process is complicated and time consuming.

Therefore, we developed a resistive pressure sensor based on a graphene/polyaniline-embedded polyvinyl butyral (GPANI-PVB) film, which is ultrathin, highly sensitive, optically transparent, anisotropically conductive, highly durable, highly flexible, and bending insensitive. The fabrication process is facile, low temperature, and all solution based. Therefore, the composite film is suitable for manufacturing low-cost and large-area touch panels. The range of variation in contact resistance and pressure sensitivity can be readily controlled by the concentration of GPANI in PVB and the thickness of the composite film. Based on the composite film, a flexible pressure-sensitive touch panel was fabricated, which supports multitouch and multilevel pressure detection.

## II. FABRICATION PROCESS

Fig. 1 shows the fabrication process of the GPANI-PVB composite film. A mixture of PVB powder, GPANI microparticles, and absolute ethyl alcohol was stirred for 4 h and subsequently ultrasonicated for another 30 min at room temperature. Because PVB is soluble in ethyl alcohol and GPANI particles can be well dispersed in a PVB-ethyl alcohol solution [22], the mixture finally became a homogenous solution. The resulting solution was coated on a patterned indium tin oxide-coated polyethylene terephthalate (ITO-PET) layer by a Mayer rod. ITO and PET served as the electrodes and substrate of pressure sensors, respectively, which can be replaced with other suitable materials. The thickness of the wet composite film (with ethyl alcohol) was approximately  $68.6 \mu\text{m}$ . After the composite film was annealed at  $80^\circ\text{C}$  for 15 min, the ethyl alcohol evaporated and the GPANI-embedded PVB film was fabricated. The thickness of the dry composite film (without ethyl alcohol) was determined by the concentration of PVB in ethyl alcohol. The thicknesses measured by a surface profiler were 1.8, 2.7, and  $3 \mu\text{m}$  for PVB concentrations of 2.5, 5, and

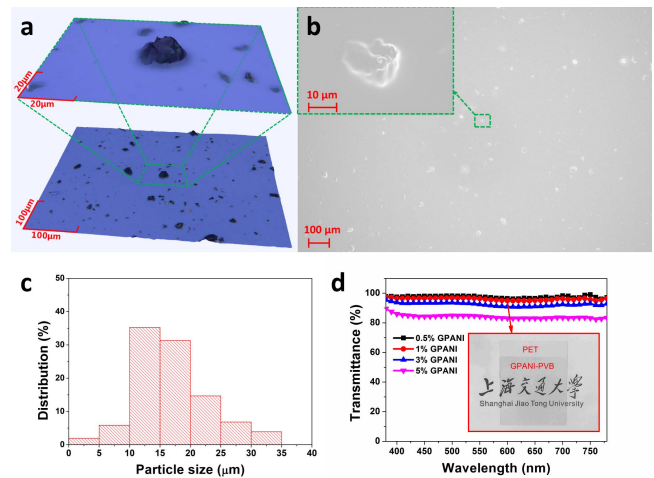


Fig. 2. Fabricated GPANI-PVB composite film. (a) and (b) Surface morphology of the composite film characterized by a 3-D optical profile and an FE-SEM, respectively. (c) Size distribution of the GPANI particles. Film thickness:  $3 \mu\text{m}$ ; concentration of GPANI in PVB: 1 wt%. (d) Transmittance of the composite film with different concentrations of GPANI in PVB. Film thickness:  $3 \mu\text{m}$ . Inset: composite film coated on a PET substrate with a GPANI concentration of 1 wt%.

10 wt%, respectively. The surface morphology of the composite film was characterized by a 3-D optical profiler [Fig. 2(a)] and a field-emission scanning electron microscope [FE-SEM, Fig. 2(b)]. The size of the GPANI particles was mainly in the range of 10–20  $\mu\text{m}$  [Fig. 2(c)], and at different positions of the PVB film, the GPANI particles showed high uniformity.

Because the size of the GPANI particles was several times larger than the thickness of the PVB film, the majority of the GPANI particles were embedded and even penetrated into the PVB film. Therefore, the composite film was conductive in the direction perpendicular to the film surface. Due to the discrete distribution of GPANI microparticles in the PVB film, the composite film was nonconductive in the direction parallel to the film surface. The anisotropic conductivity of the composite film makes it a good candidate for application in touch panels because it will not electrically connect adjacent electrodes of the same layer.

Because of the high intrinsic transmittance of the PVB film and the discrete distribution of GPANI microparticles in the PVB film, the GPANI-PVB composite film displayed high transparency [Fig. 2(d)], which can be controlled by the concentration of GPANI in the PVB film. For a GPANI concentration of less than 1 wt% in the PVB film, the composite film exhibited a uniform transmittance of more than 96% throughout the visible wavelength region (380–780 nm). This high optical transparency is a useful feature for integration of the composite film in displays. It should be noted that the size of the GPANI particles must be well controlled to be invisible to human eyes. According to Rayleigh criterion, with a viewing distance of larger than 18 cm, which is always the case for a touch panel, human eyes cannot make out particles with a size of less than  $25 \mu\text{m}$  (assuming that the minimum resolution angle of human eyes is  $0.0077^\circ$ ), which implies that the GPANI-PVB composite film is adequate for application in touch panels.

By bonding a second ITO-PET layer onto the GPANI-PVB film-covered ITO-PET by bezel tape with the ITO sides face to face, a flexible pressure-sensitive touch panel based on the composite film was fabricated. The ITO layers had been previously patterned with parallel strip electrodes with a width of 4.5 mm and a gap of 0.5 mm. The two layers of strip electrodes were arranged perpendicularly, forming a  $10 \times 10$  resistive pressure sensor array. As a comparison, a touch panel with the same two ITO-PET layers bonded together but without a GPANI-PVB composite film in between was also fabricated.

### III. PERFORMANCE OF THE RESISTIVE PRESSURE SENSORS

The bezel tape induced an ultrathin air gap between the two layers of ITO-PET. With no pressure applied, the two layers of strip electrodes were electrically insulated because of the air gap. If a finger-like rubber tip touched the panel, the top ITO layer began to contact the GPANI-PVB film on the bottom ITO layer, and conductive paths were built up. Thus, resistance could be detected at the position where the touch occurred. As the applied pressure increased from a gentle touch to a hard press, the detected resistance decreased due to the increase in contact area and the decrease in contact resistance between the GPANI particles and the two ITO layers.

Fig. 3(a) illustrates the relative change in resistance ( $\Delta R/R$ ) as a function of the applied pressure for different concentrations of GPANI in PVB. To initialize the contact between the GPANI particles and the ITO layers, the resistance detected at a pressure of 3 kPa was defined as the initial resistance. Although increasing the GPANI concentration in PVB resulted in decreased resistance, the relative variation in resistance (corresponding to the sensitivity) remained stable.

We propose a simplified model to explain the influence of GPANI concentration on sensitivity [Fig. 3(b)]. Assuming that the GPANI particles are balls of the same size, the resistance of the pressure sensor ( $R$ ) under pressure can be given by the following equation:

$$R = \frac{R_c}{A\sigma} \quad (1)$$

where  $R_c$  denotes the equivalent contact resistance resulting between one GPANI particle and the ITO layer,  $A$  denotes the contact area, and  $\sigma$  denotes the areal density of GPANI particles in the PVB film. As the applied pressure increases,  $R_c$  decreases and  $A$  increases, reducing the resistance of the pressure sensor. The relative variation in resistance can be expressed as

$$\frac{\Delta R}{R_0} = \frac{R_0 - R}{R_0} = \frac{\frac{R_{c0}}{A_0\sigma} - \frac{R_c}{A\sigma}}{\frac{R_{c0}}{A_0\sigma}} = 1 - \frac{R_c}{R_{c0}} \cdot \frac{A_0}{A} \quad (2)$$

where  $R_{c0}$  and  $A_0$  denote the equivalent contact resistance and the contact area for the initial state. The sensitivity of the pressure sensor ( $S$ ) can be defined as

$$S = \frac{\Delta R}{R_0} \cdot \frac{1}{\Delta P} = \left(1 - \frac{R_c}{R_{c0}} \cdot \frac{A_0}{A}\right) \cdot \frac{1}{\Delta P} \quad (3)$$

where  $\Delta P$  denotes the change in applied pressure. Equation (3) implies that the concentration of GPANI in PVB ( $\sigma$ ) has no effect on sensitivity. Therefore, we can achieve low power consumption for resistance measurement and meanwhile retain the high sensitivity by fabricating the pressure sensors with a low concentration of GPANI in PVB.

Based on (2), in the pressure range of 0–20 kPa, the resistance of the pressure sensor decreases sharply due to the rapid increase in contact area. In the pressure range of 20–100 kPa, the contact area remains constant (4.5 mm  $\times$  4.5 mm), and the resistance of the pressure sensor decreases more gradually because of the slow decrease in equivalent contact resistance. For a given change in contact area, the main factor affecting the sensitivity is the equivalent contact resistance between the GPANI particle and the ITO layer, which can be tuned by the size of the GPANI particles and the thickness of the composite film [Fig. 3(c)]. As the thickness of the composite film increases, the resistance of the pressure sensor increases and the sensitivity decreases, which is attributed to the fact that a thinner film has a larger relative change in equivalent contact resistance.

The pressure sensors also exhibit high durability [Fig. 3(d)]. After 7000 cycles of applying and releasing a hard press (corresponding to a pressure of approximately 100 kPa) by a finger, the resistance of the pressure sensor as a function of the applied pressure (0–100 kPa) remained stable.

Due to the influence of the bezel tape and our laboratory fabrication process, the initial resistance at different locations of the sensor array was not strictly constant and had a maximum deviation of 78.5% from the average value at a pressure of 3 kPa [Fig. 3(e)]. This will not be an issue if we employ an appropriate driving circuit which enables the measurement of large resistance variation of more than 10 times and the recording of initial resistance of the whole sensor array (see more details in Section V). Moreover, the relative change in resistance as a function of the applied pressure, which defines pressure sensitivity, was nearly the same (maximum deviation: 7.6%) [Fig. 3(f)], implying high uniformity. By well controlling the size of the GPANI particles, the variations in resistance and sensitivity may be further reduced. The high uniformity of pressure sensitivity implies that even for a large-area touch panel, the GPANI-PVB composite film is also applicable.

The pressure sensors also show a low hysteresis of less than 8.5% [Fig. 3(g)], which is lower than the hysteresis reported in [16] and [17]. The hysteresis was defined as the maximum discrepancy between the forward and backward curves divided by the full-scale resistance change. Resistive pressure sensors in the previous work usually employ elastomeric materials with microstructures as active layers and electrodes, which may suffer from viscoelastic creep due to irreversible entanglement of polymer chains with a pressure applied [9], resulting in high hysteresis. However, the pressure sensor based on the GPANI-PVB composite film relies on the change in contact area and contact resistance resulting between the more incompressible ITO-PET film and composite film [Fig. 3(b)], which yields a more reversible contact process, resulting in lower hysteresis.

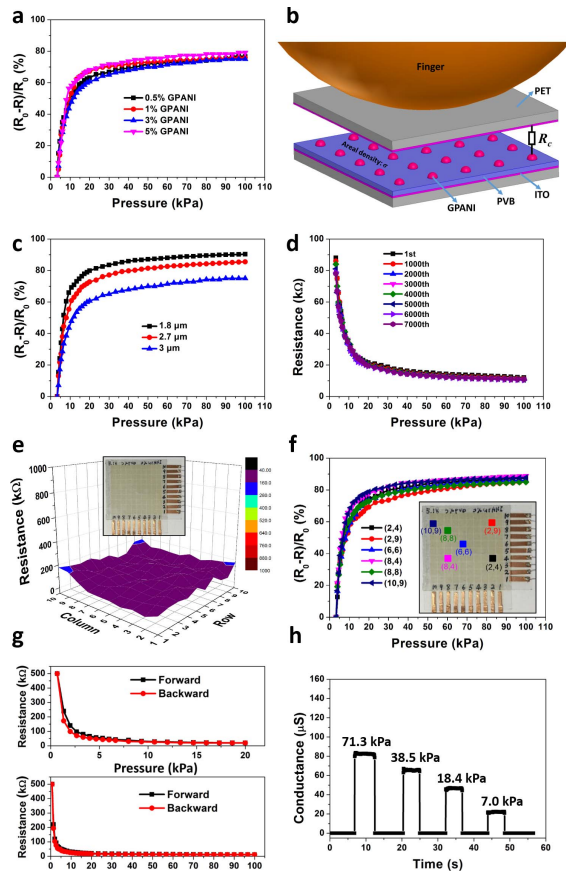


**Fig. 3.** Performance of the fabricated pressure sensors as a function of applied pressure. (a) Influence of GPANI concentration in PVB on sensitivity. Sensor position: (6, 6) in the array; film thickness: 3  $\mu\text{m}$ ; initial resistances: 660, 200, 140, and 110 k $\Omega$  for GPANI concentrations of 0.5, 1, 3, and 5 wt%, respectively. (b) Simplified model to explain the working mechanism of the pressure sensors.  $R_c$  denotes the equivalent contact resistance resulting between one GPANI particle and the ITO layer. (c) Influence of film thickness on sensitivity. Sensor position: (6, 6) in the array; concentration of GPANI in PVB: 3 wt%; initial resistances: 88, 90, and 140 k $\Omega$  for film thicknesses of 1.8, 2.7, and 3  $\mu\text{m}$ , respectively. (d) Stability and durability of the pressure sensors. A test was performed after every 1000 cycles of applying and releasing a hard press by a finger. (e) Resistance distribution of the sensor array at a pressure of 3 kPa. (f) Uniformity of the sensor array. Initial resistances: 150, 140, 90, 140, 94, and 180 k $\Omega$  for pressure sensor positions of (2, 4), (2, 9), (6, 6), (8, 4), (8, 8), and (10, 9) in the array, respectively, which represent key positions over the array. (g) Hysteresis of the pressure sensors. Two different loops (0–20–0 kPa and 0–100–0 kPa) were measured. (h) Response of the pressure sensors to different pressure levels. To include the extremely high resistance values with no pressure applied, the  $y$ -coordinate represents the conductance of the pressure sensors. For (d)–(h), film thickness: 2.7  $\mu\text{m}$ ; concentration of GPANI in PVB: 3 wt%. For (d)(g)(h), sensor position: (6, 6) in the array.

The response of the pressure sensors to different pressure levels was shown in Fig. 3(h). The test was performed by quickly applying and releasing a finger press with different pressure levels on the pressure sensors. The response and recovery time of the pressure sensors were both less than 57 ms, which was already beyond the limit of our measurement system.

Compared with resistive pressure sensors in [16], [17], and [20], the proposed pressure sensor may not have such a high sensitivity in ultralow pressure regime (less than 1 kPa), but its high sensitivity in the pressure regime of 0–100 kPa (gentle touch to hard press), high transparency,

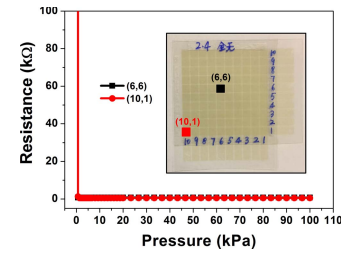


**Fig. 4.** Resistance between the two layers of strip electrodes as a function of applied pressure for the touch panel without the GPANI-PVB composite film in between.

ultrathin thickness, high stability and durability, low hysteresis, fast response (not comparable to previous work under current measurement conditions), and simplified fabrication process due to the absence of microstructures makes the pressure sensor a good candidate for application in touch panels.

#### IV. PERFORMANCE OF THE FLEXIBLE TOUCH PANEL

By directly bonding two layers of patterned ITO-PET films together without the GPANI-PVB composite film in between, a conventional resistive touch panel supporting multitouch detection was fabricated (Fig. 4) [23]. With no pressure applied, the ultrathin air gap induced by the bezel tape also results in electrical insulation between the two layers of trip electrodes. However, once a very gentle touch (less than 1 kPa) occurs on the touch panel, the resistance between the two layers of strip electrodes will sharply reduce to a very low value (several hundreds of ohms), which is mainly the resistance of ITO electrode; even if the applied pressure increases, the resistance remains nearly a constant. Therefore, the resistive touch panel without the composite film can only function as a switch and cannot detect pressure levels. Moreover, due to the ultralow ON-state resistance, the touch panel has the issue of high power consumption.

Sensor array in the touch panel with the GPANI-PVB composite film in between enables the detection of both touch position and applied pressure at the same time. Due to its high stability, the resistance of each pressure sensor in the array at a pressure of 3 kPa was recorded and set as the threshold. When a finger gently touched a certain pressure sensor, only the resistance of the touched pressure sensor was below the threshold, and the touch position was precisely identified [Fig. 5(a)]. When the finger pressed the pressure sensor hard, the resistances of the surrounding eight pressure sensors were also below the threshold because of the increase in contact area, but the relative variations in resistance did not exceed that of the central pressure sensor [Fig. 5(b)], which can precisely derive the applied pressure. Therefore, the touch panel supported multilevel pressure detection [Fig. 5(e)]. The test was performed by manually manipulating a pressure meter to successively apply multilevel pressure on the touch panel via a finger-like rubber tip. The pressure-sensitive touch panel also supported multitouch detection [Fig. 5(c) and (d)] using the positions where the peaks of the relative variation in resistance were lying. Fig. 5(a)–(d) also demonstrates from another perspective that the variation in initial resistance is not an issue due to the high uniformity of pressure sensitivity.

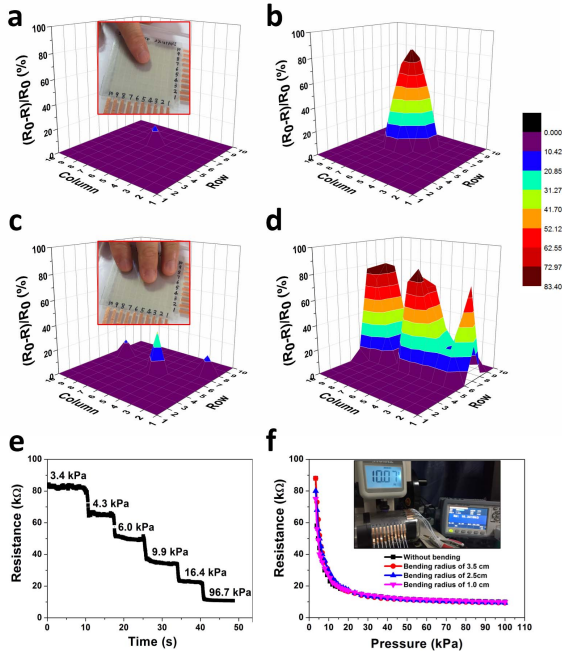


**Fig. 5.** Performance of the pressure-sensitive touch panel. (a) Gentle single touch. (b) Hard single press. (c) Gentle multitouch. (d) Hard multi-press. (e) Touch panel supports multilevel pressure detection. (f) Bending tests. Film thickness:  $2.7 \mu\text{m}$ . Concentration of GPANI in PVB: 3 wt%.

Bending tests with the touch panel attached to a curved rigid substrate were also conducted [Fig. 5(f)]. Even at a bending radius of 1 cm, the sensitivity of the touch panel remained stable due to the identical bending deformation of the two ITO-PET layers, which implies that the touch panel is bending insensitive and of high flexibility. However, because of the brittleness of ITO, the resistance of ITO-PET film has a dramatical increase with a bending radius of less than 7.5 mm, reducing the sensitivity of the touch panel. Using an ITO-replacement material of higher flexibility, such as silver nanowires and metal mesh [24]–[27], the bending insensitivity, and flexibility of the touch panel may be improved.

Compared with conventional resistive touch panel without the composite film, the proposed touch panel can not only support multilevel pressure detection, but also reduce the power consumption due to the controllable contact resistance (in the level of tens to hundreds of kilohms). Compared with current pressure-sensitive touch technologies [4], [5], [21], the proposed touch panel combines the detection of both touch position and pressure, and has high noise immunity due to resistance measurement, enabling its application in harsh circumstances, such as under water or in intense electromagnetic fields; it is also bending insensitive and of high flexibility, and can support multitouch and multilevel pressure detection.

## V. DISCUSSION

For practical use, the influence of temperature and humidity on the performance of the touch panel should be considered. Although humidity has a negligible effect on the performance [Fig. 6(a)], an increase in temperature results in a nearly linear reduction in the resistance of the pressure

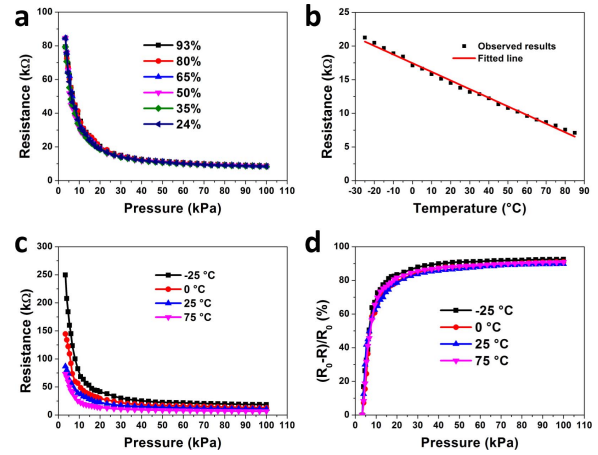


**Fig. 6.** Influence of humidity and temperature on the performance of the touch panel. (a) Change in sensor resistance as a function of applied pressure with different relative humidities. Temperature: 22 °C. (b) Change in sensor resistance as a function of temperature with an applied pressure of 50 kPa. (c) Change in sensor resistance as a function of applied pressure with different temperatures. (d) Relative change in sensor resistance as a function of applied pressure with different temperatures. Relative humidity: 45%. Sensor position: (6, 6) in the array; film thickness:  $2.7 \mu\text{m}$ ; concentration of GPANI in PVB: 3 wt%.

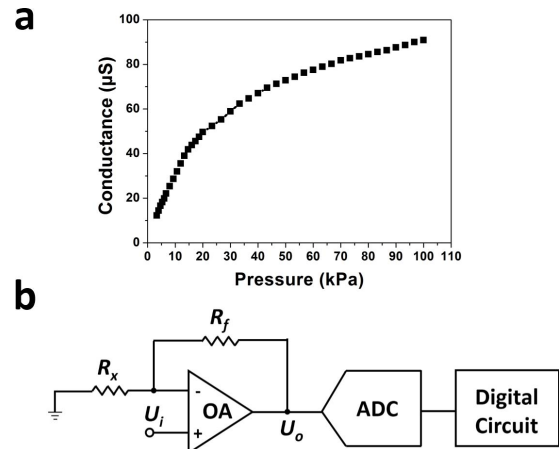


**Fig. 7.** Solution to the relatively low sensitivity of the pressure sensors in the pressure range of 20–100 kPa. (a) Conductance change of the pressure sensors as a function of applied pressure. (b) Driving circuit transforming the measurement of resistance change into output voltage change.

sensors [Fig. 6(b) and (c)]. The resistance variation may be attributed to the fact that an increase in temperature results in a reduction in the equivalent contact resistance between the GPANI particle and the ITO layer, considering that only a slight increase (2.1%) in the resistance of ITO-PET film is induced by an increase in temperature from  $-25 \text{ }^\circ\text{C}$  to  $85 \text{ }^\circ\text{C}$ . However, the relative change in resistance (representing the sensitivity) remains stable [Fig. 6(d)]. Therefore, the temperature-induced resistance variation can be calibrated if we fabricate a similar sensor based on the GPANI-PVB film with a given pressure (such as 3 kPa) in the touch panel and measure its resistance as the threshold value.

Fig. 3 shows that in the pressure range of 20–100 kPa, the pressure sensors have a relatively low sensitivity due to the nearly constant contact area and the slow decrease

in equivalent contact resistance. However, situation can be much improved if we use the change in conductance, which is the reciprocal of resistance, to identify the applied pressure [Fig. 7(a)]. The improvement is due to the approximately inverse proportional relationship between the resistance of pressure sensors and the applied pressure (20–100 kPa) (Fig. 3). Fig. 7(b) illustrates a measurement circuit making use of the conductance change. According to the principle of noninverting operational amplifier (OA) with a negative feedback, the output voltage ( $U_o$ ) can be expressed as

$$U_o = U_i \left( 1 + \frac{R_f}{R_x} \right) \quad (4)$$

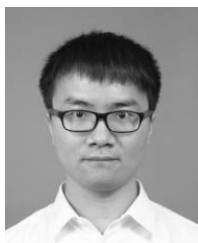
where  $U_i$  denotes the input voltage,  $R_f$  denotes the feedback resistance, and  $R_x$  denotes the resistance of pressure sensors to be measured. With no pressure applied,  $R_x$  is infinite and  $U_o = U_i$  and as the applied pressure increases,  $R_x$  decreases and  $U_o$  increases.  $R_x = R_f$  yields  $U_o = 2U_i$  and  $R_x = R_f/N$  under a high pressure yields  $U_o = (N + 1)U_i$ . Therefore, the driving circuit transforms the measurement of resistance change into output voltage change which is a linear function of the conductance of pressure sensors, improving the pressure sensitivity in the pressure range of 20–100 kPa. Moreover, the change in output voltage can be conveniently processed by back-end digital circuits via an analog-to-digital converter.

## VI. CONCLUSION

The high sensitivity, high transparency, high flexibility, high uniformity, low hysteresis, fast response time, anisotropic conductivity, and bending insensitivity of the GPANI-PVB composite film make it a good candidate for fabricating flexible interactive electronic devices, such as flexible displays, transparent electronic skins, and health monitors. These devices can provide users or robotics with information regarding both the contact position and the applied pressure. Because these devices work by detecting resistance instead of capacitance, the influence of electromagnetic interference on measurement results is negligible, implying that these devices will show high reliability and applicability under harsh circumstances, such as under water or in intense electromagnetic fields. The facile, low-temperature, and all-solution-based method also enables the fabrication of low-cost, large-area interactive devices.

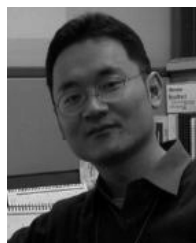
## REFERENCES

- [1] J. Kim *et al.*, "Stretchable silicon nanoribbon electronics for skin prosthesis," *Nature Commun.*, vol. 5, p. 5747, Dec. 2014.
- [2] D.-H. Kim *et al.*, "Epidermal electronics," *Science*, vol. 333, no. 6044, pp. 838–843, 2011.
- [3] A. Chortos, J. Liu, and Z. Bao, "Pursuing prosthetic electronic skin," *Nature Mater.*, vol. 15, pp. 937–950, Jul. 2016.
- [4] D. J. Lipomi *et al.*, "Skin-like pressure and strain sensors based on transparent elastic films of carbon nanotubes," *Nature Nanotechnol.*, vol. 6, pp. 788–792, Oct. 2011.
- [5] M. Ando, H. Kawamura, H. Kitada, Y. Sekimoto, T. Inoue, and Y. Tajitsu, "Pressure-sensitive touch panel based on piezoelectric poly(L-lactic acid) film," *Jpn. J. Appl. Phys.*, vol. 52, no. 9S1, p. 09KD17, Sep. 2013, doi: 10.7567/jjap.52.09kd17.
- [6] S. Chen, B. Zhuo, and X. Guo, "Large area one-step facile processing of microstructured elastomeric dielectric film for high sensitivity and durable sensing over wide pressure range," *ACS Appl. Mater. Interfaces*, vol. 8, no. 31, pp. 20364–20370, 2016.
- [7] H. Vandeparre, D. Watson, and S. P. Lacour, "Extremely robust and conformable capacitive pressure sensors based on flexible polyurethane foams and stretchable metallization," *Appl. Phys. Lett.*, vol. 103, no. 20, p. 204103, 2013.
- [8] Y. Joo *et al.*, "Silver nanowire-embedded PDMS with a multiscale structure for a highly sensitive and robust flexible pressure sensor," *Nanoscale*, vol. 7, no. 14, pp. 6208–6215, 2015.
- [9] S. C. B. Mannsfeld *et al.*, "Highly sensitive flexible pressure sensors with microstructured rubber dielectric layers," *Nature Mater.*, vol. 9, pp. 859–864, Sep. 2010.
- [10] I. Graz *et al.*, "Flexible active-matrix cells with selectively poled bifunctional polymer-ceramic nanocomposite for pressure and temperature sensing skin," *J. Appl. Phys.*, vol. 106, no. 3, p. 034503, Aug. 2009, doi: 10.1063/1.3191677.
- [11] L. Persano *et al.*, "High performance piezoelectric devices based on aligned arrays of nanofibers of poly(vinylidene fluoride-co-trifluoroethylene)," *Nature Commun.*, vol. 4, Mar. 2013, Art. no. 1633, doi: 10.1038/ncomms2639.
- [12] M. Akiyama *et al.*, "Flexible piezoelectric pressure sensors using oriented aluminum nitride thin films prepared on polyethylene terephthalate films," *J. Appl. Phys.*, vol. 100, no. 11, p. 114318, 2006.
- [13] S. Jung *et al.*, "Reverse-micelle-induced porous pressure-sensitive rubber for wearable human-machine interfaces," *Adv. Mater.*, vol. 26, no. 28, pp. 4825–4830, May 2014, doi: 10.1002/adma.201401364.
- [14] X. Wang, Y. Gu, Z. Xiong, Z. Cui, and T. Zhang, "Silk-molded flexible, ultrasensitive, and highly stable electronic skin for monitoring human physiological signals," *Adv. Mater.*, vol. 26, no. 9, pp. 1336–1342, Mar. 2014.
- [15] M. Amjadi, A. Pichitpajongkit, S. Lee, S. Ryu, and I. Park, "Highly stretchable and sensitive strain sensor based on silver nanowire-elastomer nanocomposite," *ACS Nano*, vol. 8, no. 5, pp. 5154–5163, Apr. 2014, doi: 10.1021/nn501204t.
- [16] C.-L. Choong *et al.*, "Highly stretchable resistive pressure sensors using a conductive elastomeric composite on a micro pyramid array," *Adv. Mater.*, vol. 26, no. 21, pp. 3451–3458, Jun. 2014, doi: 10.1002/adma.201305182.
- [17] L. Pan *et al.*, "An ultra-sensitive resistive pressure sensor based on hollow-sphere microstructure induced elasticity in conducting polymer film," *Nature Commun.*, vol. 5, p. 3002, Jan. 2014.
- [18] B. C.-K. Tee, C. Wang, R. Allen, and Z. Bao, "An electrically and mechanically self-healing composite with pressure- and flexion-sensitive properties for electronic skin applications," *Nature Nanotechnol.*, vol. 7, no. 12, pp. 825–832, Nov. 2012, doi: 10.1038/nnano.2012.192.
- [19] I. Rosenberg and K. Perlin, "The UnMousePad: An interpolating multi-touch force-sensing input pad," *ACM Trans. Graph.*, vol. 28, no. 3, Aug. 2009, Art. no. 65, doi: 10.1145/1531326.1531371.
- [20] S. Lee *et al.*, "A transparent bending-insensitive pressure sensor," *Nature Nanotechnol.*, vol. 11, pp. 472–478, Jan. 2016.
- [21] Z. Chen *et al.*, "Enhancing the sensitivity of percolative graphene films for flexible and transparent pressure sensor arrays," *Adv. Funct. Mater.*, vol. 26, no. 28, pp. 5061–5067, 2016.
- [22] Y. Li, T. Yu, T. Pui, P. Chen, L. Zheng, and K. Liao, "Fabrication of transparent and conductive carbon nanotube/polyvinyl butyral films by a facile solution surface dip coating method," *Nanoscale*, vol. 3, no. 6, pp. 2469–2471, Jun. 2011, doi: 10.1039/c1nr10302d.
- [23] G. Walker, "A review of technologies for sensing contact location on the surface of a display," *J. Soc. Inf. Display*, vol. 20, no. 8, pp. 413–440, Jun. 2012, doi: 10.1002/jsid.100.
- [24] A. R. Madaria, A. Kumar, and C. Zhou, "Large scale, highly conductive and patterned transparent films of silver nanowires on arbitrary substrates and their application in touch screens," *Nanotechnology*, vol. 22, no. 24, p. 245201, 2011.
- [25] L. Hu, H. S. Kim, J.-Y. Lee, P. Peumans, and Y. Cui, "Scalable coating and properties of transparent, flexible, silver nanowire electrodes," *ACS Nano*, vol. 4, no. 5, pp. 2955–2963, 2010.
- [26] J. Y. Lee, S. T. Connor, Y. Cui, and P. Peumans, "Solution-processed metal nanowire mesh transparent electrodes," *Nano Lett.*, vol. 8, no. 2, pp. 689–692, 2008.
- [27] M.-G. Kang, H. J. Park, S. H. Ahn, and L. J. Guo, "Transparent Cu nanowire mesh electrode on flexible substrates fabricated by transfer printing and its application in organic solar cells," *Solar Energy Mater. Solar Cells*, vol. 94, no. 6, pp. 1179–1184, Mar. 2010, doi: 10.1016/j.solmat.2010.02.039.



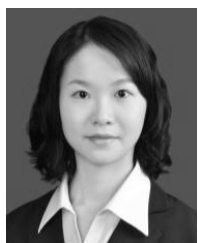
**Shi-Yu Liu** received the B.S. degree from the Department of Information Science and Electronic Engineering, Zhejiang University, Hangzhou, China, in 2011. He is currently pursuing the Ph.D. degree with the National Engineering Laboratory for TFT-LCD Materials and Technologies, Department of Electronic Engineering, Shanghai Jiao Tong University, Shanghai, China.

His current research interests include touch sensors and pressure sensors.



**Jian-Gang Lu** received the Ph.D. degree from the College of Information Science and Engineering, Zhejiang University, Hangzhou, China, in 2003.

Since 2009, he has been an Associate Professor with the National Engineering Laboratory for TFT-LCD Materials and Technologies, Shanghai Jiao Tong University, Shanghai, China. His current research interests include liquid crystal material, polymer material, liquid crystal display mode, and 3-D display.



**Lu Lian** received the master's degree from the Department of Material Science and Engineering, Xi'an Jiao Tong University, Xi'an, China. She is currently pursuing the Ph.D. degree with the National Engineering Laboratory for TFT-LCD Materials and Technologies, Department of Electronic Engineering, Shanghai Jiao Tong University, Shanghai, China, with a focus on high-quality silver and copper nanowire synthesis, fabrication of high-performance flexible transparent composite electrodes, and exploring their

applications in organic light-emitting diodes.



**Jin Pan** received the B.S. degree from the Department of Electronic Engineering, Shanghai Jiao Tong University, Shanghai, China, in 2017, where he is currently pursuing the M.S. degree with the National Engineering Laboratory for TFT-LCD Materials and Technologies, Department of Electronic Engineering.

His current research interests include touch and interactive technologies.



**Han-Ping D. Shieh** (F'08) received the Ph.D. degree in electrical and computer engineering from Carnegie Mellon University, Pittsburgh, PA, USA., in 1987.

He founded and served as the Director at the Display Institute, NCTU in 2003. He is currently an NCTU Chair Professor. He has been holding an appointment as a Chang Jiang Scholar at Shanghai Jiao Tong University, Shanghai, China, since 2010.